Journal of Cardiovascular Computed Tomography xxx (xxxx) xxx

Contents lists available at ScienceDirect

Journal of Cardiovascular Computed Tomography

journal homepage: www.JournalofCardiovascularCT.com

Research paper

Geometric differences of the mitral valve apparatus in atrial and ventricular functional mitral regurgitation

Anna Reid, Sagit Ben Zekry, Christopher Naoum, Hidenobou Takagi, Christopher Thompson, Marcelo Godoy, Malcolm Anastasius, Stephanie Tarazi, Mansi Turaga, Robert Boone, John Webb, Jonathon Leipsic, Philipp Blanke *

Center for Heart Valve Innovation/Department of Radiology, St. Paul's Hospital, University of British Columbia, Vancouver, BC, Canada

ARTICLE INFO

Keywords:
Functional mitral regurgitation
Atrial mitral regurgitation
Mitral annulus
Left ventricular geometry
Transcatheter mitral valve implantation
Cardiac computed tomography

ABSTRACT

Background: Functional mitral regurgitation (FMR) occurs in patients with annular dilation (atrial, aFMR) or patients with left ventricular (LV) disease (ventricular, vFMR). Meticulous understanding of the mechanisms underpinning regurgitation is crucial to optimize therapeutic strategies.

Methods: Patients with moderate-severe FMR were identified from a registry of patients referred for transcatheter mitral valve intervention. In addition, controls without cardiovascular disease were identified. Differences in the geometry of the LV and mitral valve apparatus (including leaflet and tenting geometry, papillary muscle displacement and movement, annular dimensions, and dynamism) between atrial and ventricular FMR, and control subjects, were assessed using multiphasic cardiac CT.

Results: Of 183 FMR patients, 18 patients (10%) were found to have aFMR. The remaining patients had either ischemic or non-ischemic ventricular FMR. In aFMR, both increasing LV end-systolic volume (rho 0.701, $p < 0.01$) and left atrial volume (rho 0.909, $p < 0.01$) were associated with larger annular area. By contrast, in vFMR larger annular area was most strongly associated with larger left atrial volume (rho 0.63, $p < 0.01$). In controls, increased annular area was associated with larger LVEDV (rho 0.78, $p < 0.01$) and LVESV (rho 0.824, $p < 0.01$), but not left atrial size (rho 0.16, $p = 0.45$).

Ventricular FMR comprised apicolaterally displaced, akinetic posteromedial papillary muscles, resulting in pronounced leaflet tethering, leaflet elongation compared to controls, and only modest relative LA dilatation. Compared to vFMR, aFMR was characterised by marked relative annular dilation, smaller but discernible mitral valve tenting, shorter leaflet lengths when related to annular size, but normal papillary geometry.

Conclusion: FMR is characterised by multiple changes within the mitral valve complex. Atrial and ventricular FMR differ significantly in terms of the drivers of annular size, and geometry and function of the subvalvular apparatus. This highlights the need to consider these as separate disease entities.

1. Introduction

Functional mitral regurgitation (FMR) affects approximately one-third of patients with ischemic- or non-ischemic dilated cardiomyopathy and is associated with adverse outcomes.[1] Typically, *ventricular* FMR has been considered in relation to geometric changes to the left ventricle (LV). Our understanding of the complex mechanisms underpinning ventricular FMR has been greatly advanced by 3-dimensional echocardiography (3DE), highlighting key features of the distortion and dysfunction of the valvular and subvalvular mitral valve (MV) apparatus, including leaflet tethering, inadequate leaflet remodelling, papillary muscle (PM) displacement, and mitral annular (MA) dilatation.[2] *Atrial* FMR has historically been less appreciated, and typically occurs in the context of atrial fibrillation (AF), with left atrial (LA) dilatation, and preserved LV geometry and ejection fraction (EF).[3] Isolated annular dilatation has previously been considered the mechanism for atrial FMR. However, recent evidence suggests that atriogenic (rather than ventricular) leaflet tethering, inadequate leaflet remodelling and loss of atrial dynamism are fundamental drivers of atrial FMR.[4–6]

Numerous transcatheter approaches targeting different components of the mitral valve apparatus have been developed for treatment of mitral regurgitation. CT is an essential component of the pre-procedural planning of these procedures, through the granular assessment of the

* Corresponding author. Center for Heart Valve Innovation/Department of Radiology, St. Paul's Hospital, University of British Columbia, Vancouver, BC, Canada.
E-mail address: phil.blanke@gmail.com (P. Blanke).

https://doi.org/10.1016/j.jcct.2022.02.008
Received 26 April 2021; Received in revised form 13 January 2022; Accepted 21 February 2022
Available online xxxx
1934-5925/

Abbreviations

3DE	3-Dimensional echocardiography
AF	Atrial fibrillation
ALPM	Anterolateral papillary muscle
AMVL	Anterior mitral valve leaflet
BSA	Body surface area
CT	Computed tomography
ECG	Electrocardiogram
EF	Ejection fraction
EROA	Effective regurgitant orifice area
FMR	Functional mitral regurgitation
IC	Intercommissural
LA	Left atrial
LV	Left ventricular
LVEDV (i)	Left ventricular end diastolic volume (indexed)
LVESV (i)	Left ventricular end systolic volume (indexed)
LVSV (i)	Left ventricular stroke volume (indexed)
MA	Mitral annular
MI	Myocardial infarction
MPR	Multiplanar reformat
MR	Mitral regurgitation
MV	Mitral valve
PISA	Proximal isovelocity surface area
PM	Papillary muscle
PMPM	Posteromedial papillary muscle
PMVL	Posterior mitral valve leaflet
RegF	Regurgitant fraction
RegV	Regurgitant volume
SL	Septo-lateral
TEE	Transesophageal echocardiogram
TMVI	Transcatheter mitral valve intervention
TTE	Transthoracic echocardiogram

underlying anatomy, and thus may provide insights into the mechanisms driving regurgitation in individual patients. We therefore sought to elaborately interrogate the geometry of the mitral valve apparatus, annular dimensions, and drivers of annular size in patients with moderate to severe atrial and ventricular FMR, compared to control subjects, using retrospectively electrocardiographically (ECG) gated cardiac CT.

2. Methods

2.1. Patient population

Two study cohorts were included into this study, 183 patients with FMR and 25 controls. FMR patients were identified from a retrospective database of 422 patients with moderate to severe mitral regurgitation (MR) being referred to the transcatheter heart valve program at St. Paul's Hospital for potential transcatheter mitral valve intervention (TMVI) between 2014 and 2020 (Fig. 1). Patients included into this database had undergone a clinical cardiac CT with acquisition protocol tailored to mitral assessment. This CT time-point represented the 'index-time'; baseline variables relate to this time point. Definitions for clinical comorbidities were as per the COAPT trial.[7] The principal inclusion criterion for this study was the presence of FMR. Exclusion criteria included any other cause of MR, and previous mitral valve intervention. Controls were randomly identified from a previously analysed and described cohort by our group,[8] as being free of significant cardiac disease on the basis of CT findings and review of available clinical information.

Retrospective analysis of the clinical transthoracic echocardiogram (TTE) that related to the initial referral was performed. The mechanism of MR and etiology of LV dysfunction was determined by consensus review (SB/ABR/MT/PB) of TTE and transesophageal echocardiographic (TEE) and CT, but blinded to other clinical data. Atrial FMR was defined as MR in the context of no discernible primary MV abnormality on TTE and TEE, atrial and annular dilatation, and no discernible LV pathology (i.e., normal LV size and ejection fraction with no regional wall motion abnormality, and quantitatively assessed ejection fraction >45% on CT). All subsequent image analysis was performed blinded to all clinical data. This retrospective study was approved by the Institutional Review Board with a waiver for informed consent.

2.2. Echocardiographic data acquisition and analysis

All echocardiographic studies were performed as part of routine clinical care (predominantly iE33, Phillips, Leiden). Images were stored digitally for future analysis. Mitral valve geometry was analysed from the mid-esophageal long-axis view (TEE) in mid diastole for leaflet length (hinge point to tip), and peak systole for tenting assessment.

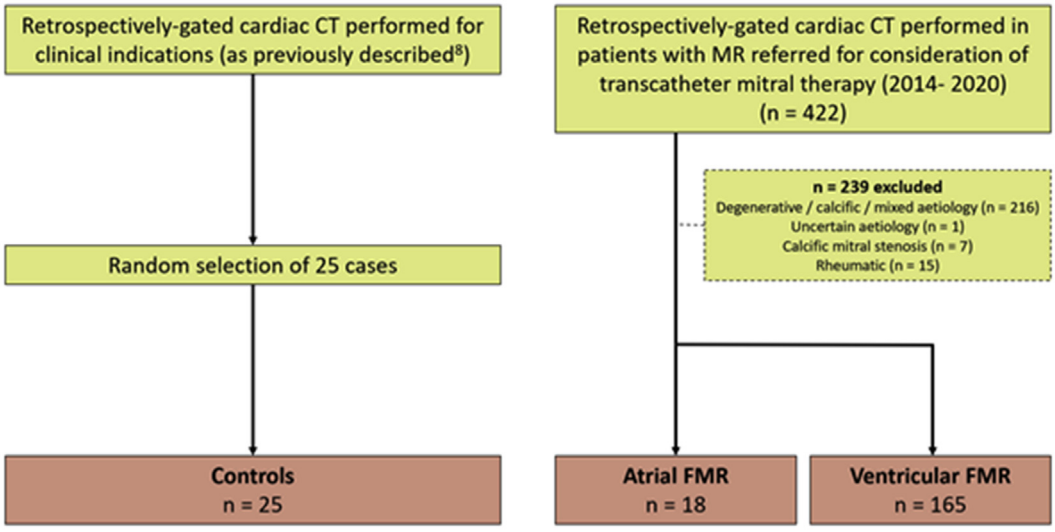

Fig. 1. Study Flow Chart. Patients included in the control and functional mitral regurgitation (FMR) cohorts, and reasons for exclusion.

Retrospective analysis and quantification were performed from TTE by a single observer (SB) blinded to all clinical data (Tomtec Cardiac Performance Analysis version 1.3.0.91, CPA, Tomtec, Unterschleissheim, Germany). Mitral regurgitation was quantified using the proximal isovelocity surface area (PISA) method including the effective regurgitant orifice area (EROA) and regurgitant volume and fraction (RegV/RegF), as per American Society of Echocardiography recommendations.[9]

2.3. Cardiac CT data acquisition and analysis

Cardiac CT was performed using a 64-slice helical CT scanner (GE Discovery high-definition 750 or VCT), after September 2015 using a 256-slice volume CT scanner (GE Revolution, GE Healthcare, Milwaukee, Wisconsin). Data acquisition was performed during a single breath-hold following injection of approximately 80 ml of intravenous contrast media (Visipaque320, GE Healthcare) with a biphasic injection (contrast and saline). Tube-voltage and current were adjusted to body habitus. Scan range extended from the carina to just below the inferior cardiac surface. Axial images were reconstructed at 10% intervals of the cardiac cycle with a slice thickness of 0.625 mm.

LV and left atrial (LA) volumes were determined using a commercially available, threshold-based, 3D segmentation algorithm with manual correction (Aquarius iNtuition v4.4.12, TeraRecon, Foster City, California). LV end diastolic volumes (LVEDV), end systolic volumes (LVESV), and stroke volumes (LVSV) were indexed to body surface area (BSA) using the Mosteller formula (LVEDVi, LVESVi and LVSVi, respectively). Dynamism was determined by the difference in systolic and diastolic LA area and sphericity. LV sphericity was calculated as the ratio of diastolic LV diameter to length.

Segmentation of the D-shaped mitral annulus (MA) was performed in end-systole and end-diastole as previously described[10] using Circle CVI (Circle Cardiovascular Imaging, Calgary, AB), yielding area, perimeter, inter-commissural (IC) and septal-to-lateral (SL) diameters. MA sphericity was calculated as the ratio of the SL to IC distance.

Mitral valve leaflet lengths were assessed on the 3-chamber view in mid-diastole, measured from the annular plane to leaflet tip, similar to echocardiographic methods. Tenting height, area and leaflet angles were measured at end systole in the same view (Fig. 2).[11] Papillary muscle analysis is described in Fig. 3.

2.4. Statistical analysis

Analysis was performed using SPSS version 23.0 (SPSS, Chicago, IL, USA). Discrete data are presented as frequency and percentage. Continuous data are presented as mean ± standard deviation, or median and interquartile range, for normally distributed and non-normally distributed data, respectively. Normality was determined using the Kolmogorov-Smirnov method. Differences between unpaired groups were analysed using the unpaired Student *t*-test and Mann–Whitney *U*

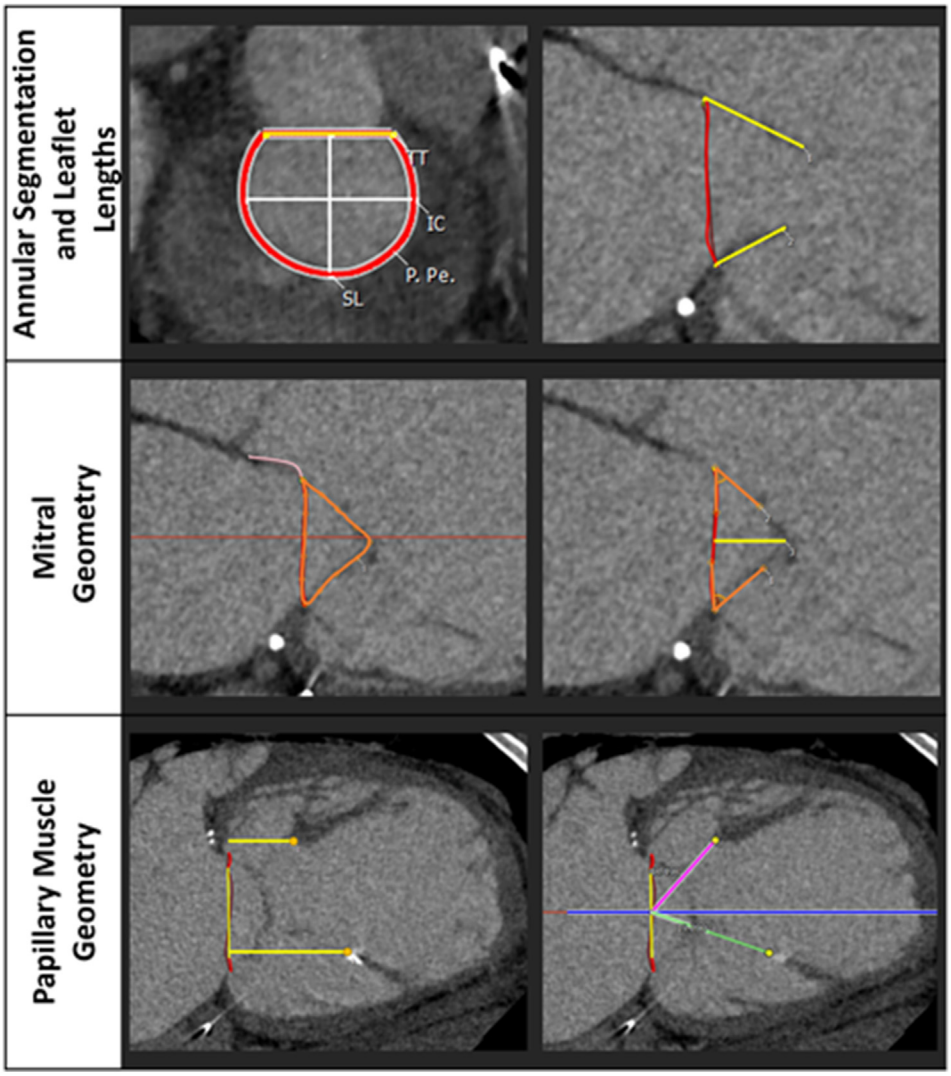

Fig. 2. Annular, mitral valve and papillary muscle analysis. **A**, Annular segmentation was performed in end-diastole and end-systole,[5] represented in red throughout figure. **B**, Leaflet lengths (yellow lines) were determined using multiplanar reformat (MPR) at A2 and P2 segments. **C** and **D**, Tenting area and angles were measured, with the area enclosed between the atrial surface of the valve leaflets to the level of the coaptation point (yellow arrows) and the annular plane (orange segmentation). Tenting height was measured as the perpendicular distance between the annular plane and the coaptation point (yellow line, D). **E**, The distance from the annular plane to the most proximal, dominant head of the anterolateral and posteromedial papillary muscles were measured in a perpendicular fashion to the annular plane. **F**, The angulation of 3D trajectories from the geometric centre of the annulus to the papillary muscle heads was assessed in relation to the mitral annular trajectory. (For interpretation of the references to colour in this figure legend, the reader is referred to the Web version of this article).

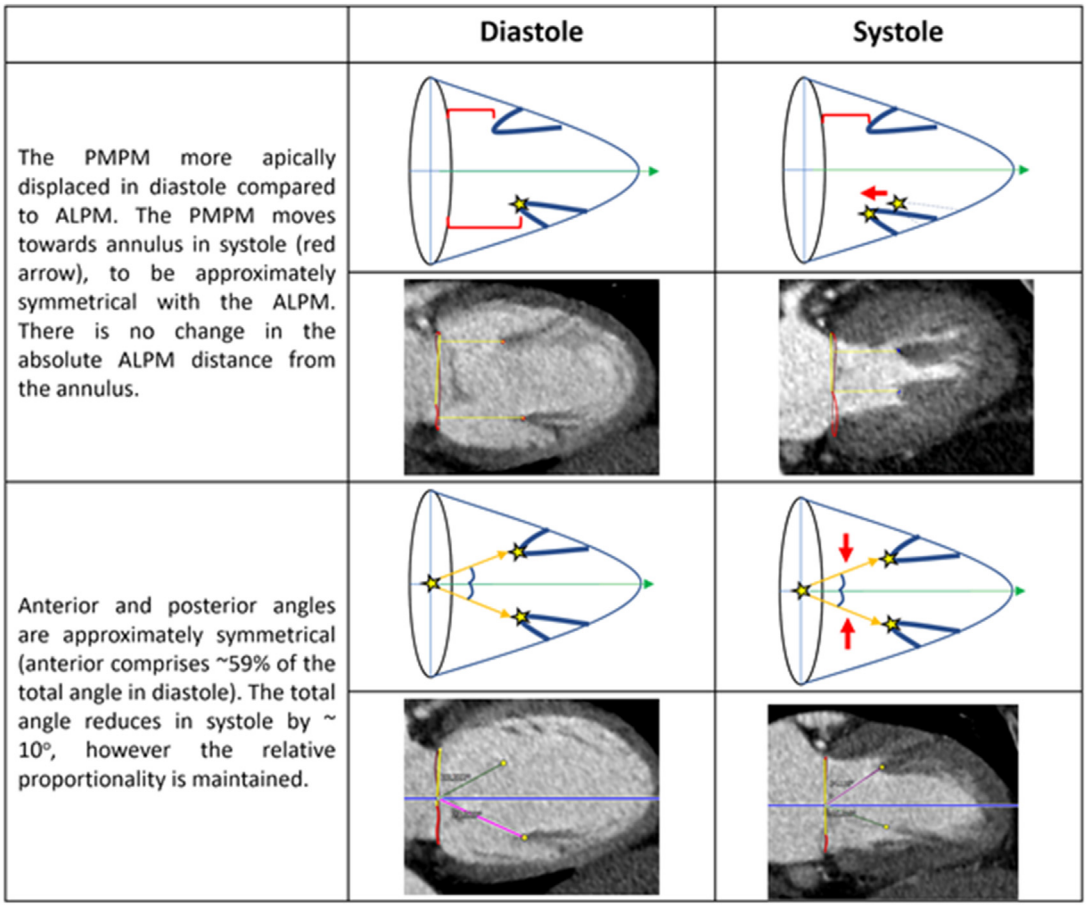

Fig. 3. Normal papillary muscle geometry in diastole and systole.

test was used where continuous data displayed normal and skewed distribution, respectively. Paired data was compared using paired Student *t*-test. Pearson χ^2 test was used for non-continuous data. Correlations were performed using Spearman Rank correlation coefficient (non-normal continuous data).

In order to investigate the relative contribution of changes in LA and LV sizes in ventricular FMR, univariate predictors of MA area indexed to BSA were evaluated using Pearson correlation. Multivariable linear regression was subsequently performed including univariate predictors in the model (entry criteria $p < 0.1$). Where two covariates strongly correlated ($R \geq 0.70$), the variable with more significant univariate association was included to avoid collinearity. Multicollinearity was assessed as tolerance values greater than 0.1. Unstandardized and standardized beta coefficients are reported for individual variables, and the adjusted R^2 is reported for the overall model.

3. Results

3.1. Patient population

Of the 183 patients with FMR, 165 patients were adjudicated as having ventricular FMR (75 non-ischemic dilated cardiomyopathy, 90 ischemic cardiomyopathy), and 18 patients as having aFMR (10% of the total cohort, Fig. 1). Baseline characteristics are presented in Table 1. Overall, FMR patients were multimorbid, were frequently symptomatic (62% NHYA III or IV) and had severely enlarged and impaired ventricles (median LVEDVi 135 ml/m^2 (93–178ml/m2); mean LV EF 46 ± 14%). No statistically significant difference in regurgitant fraction was seen between atrial and ventricular FMR. Control patients were younger, 48% were male.

3.2. Left ventricular and atrial geometry

As expected, indexed LV volumes were significantly larger and LVEF lower in patients with ventricular FMR compared to atrial FMR and controls (median 152 ml/m^2, IQR 119–189 ml/m^2 vs. 78 ml/m^2, IQR 66–113 ml/m^2, and 59 ml/m^2, IQR 52–66 ml/m^2, respectively, $p < 0.01$). LA volumes in both atrial and ventricular FMR were significantly larger compared to controls (median 105 ml/m^2, IQR 85–129 ml/m^2 vs. 45 ml/m^2, 40–49 ml/m^2, $p < 0.01$). Whilst no difference in indexed LA volume was observed between atrial and ventricular FMR, the ratio of LA to LVEDV was significantly higher in patients with atrial FMR compared to ventricular FMR (median 1.32, IQR 1.01–2.18 vs. 0.67, IQR 0.52–0.87, $p < 0.01$) and controls (0.75, IQR 0.63–0.94, $p < 0.01$).

3.3. Mitral annular dimensions

The range of absolute annular areas observed is shown as histograms in Fig. 4. Absolute annular dimensions were similar in atrial and ventricular FMR, but significantly larger than controls (Table 2). When indexed to LV volume, however, MA area in patients with ventricular FMR was significantly smaller than aFMR and controls, which were similar. When indexed to LA volume, MA area was significantly lower in both ventricular and atrial FMR compared to controls, particularly in atrial FMR.

Associations between absolute MA area and LV and LA volumes are illustrated in Fig. 5. In patients with atrial FMR, increasing MA area was univariately associated with increasing LA volume (rho 0.909, $p < 0.01$), and to a lesser degree, increasing LVESV (rho 0.701, $p < 0.01$). Multivariate analysis was not performed due to the small sample size. For ventricular FMR, univariate and multivariate predictors of indexed MA area

Table 1
Baseline characteristics of all subgroups (definitions for comorbidities as per the COAPT trial.[7] Data is presented as mean ± standard deviation, or median and interquartile range).

Clinical Characteristics	All FMR n = 183	Ventricular FMR n = 165	Atrial FMR n = 18	Controls n = 25 (%)
Age (years)	73 ± 12	72 ± 12	80 ± 6[c]	55 ± 10
Male	73 ± 11	72 ± 11	81 ± 6	54 ± 11
Female	72 ± 13	71 ± 13	80 ± 5	55 ± 9
Sex (male)	116 (63%)	110 (67%)	6 (33%)	12 (48%)
BSA (m^2)	1.86 ± 0.27	1.87 ± 0.27	1.82 ± 0.29	1.90 ± 0.25
Male	1.93 ± 0.25	1.93 ± 0.25	1.99 ± 0.25	2.03 ± 0.23
Female	1.75 ± 0.25	1.75 ± 0.25	1.74 ± 0.28	1.79 ± 0.18
eGFR(ml/min/1.73m^2)	51 ± 21	51 ± 21	55 ± 15	NA
Male	52 ± 21	51 ± 21	55 ± 12	
Female	50 ± 21	48 ± 21	56 ± 17	
NTproBNP (pg/mL)	1897 (768–3798)	1948 (774–3732)	1429 (636–8051)	NA
NYHA I	6 (3%)	5 (3%)	1 (6%)	NA
II	63 (34%)	57 (35%)	6 (33%)	
III	103 (56%)	93 (56%)	10 (56%)	
IV	11 (6%)	10 (6%)	1 (6%)	
Stroke/TIA	15 (8%)	12 (7%)	3 (17%)	NA
Peripheral Vascular Disease	6 (3%)	3 (2%)	3 (17%)[c]	NA
Diabetes	44 (24%)	41 (25%)	3 (17%)	NA
Hypertension	101 (55%)	87 (53%)	14 (78%)[c]	NA
Raised cholesterol	99 (54%)	91 (55%)	8 (44%)	NA
Atrial Fibrillation/Flutter	113 (62%)	95 (58%)	18 (100%)[c]	NA
Chronic Kidney Disease	70 (38%)	67 (41%)	3 (17%)[c]	NA
Anemia	11 (6%)	9 (6%)	2 (11%)	NA
COPD	33 (18%)	30 (18%)	3 (17%)	NA
LV EDVi (ml/m^2)	141 (114–183)	152 (119–189)	78 (66–113)[c]	59 (52–67)[a,b]
Male	154 (128–195)	156 (130–206)	113 (90–128)[c]	55 (46–64)[a,b]
Female	118 (86–164)	129 (107–183)	76 (58–86)[c]	63 (54–71)[a,b]
LV ESVi (ml/m^2)	95 (66–128)	102 (74–141)	37 (26–55)[c]	20 (17–26)[a,b]
Male	104 (79–145)	110 (82–148)	56 (51–59)[c]	19 (16–26)[a,b]
Female	72 (51–118)	81 (63–127)	27 (26–38)[c]	22 (17–27)[a,b]
LV SVi (ml/m^2)	48 ± 14	48 ± 14	48 ± 15	38 ± 6[a,b]
Male	49 ± 15	49 ± 15	55 ± 15	35 ± 5[a]
Female	45 ± 13	46 ± 12	44 ± 14	41 ± 5[a,b]
LV EF (%)	35 ± 13	33 ± 11	55 ± 10[c]	65 ± 7[a,b]
Male	33 ± 12	32 ± 11	50 ± 5[c]	63 ± 6[a,b]
Female	39 ± 14	35 ± 10	57 ± 11[c]	67 ± 7[a,b]
LA Voli (ml/m^2)	105 (85–129)	105 85–127)	106 (81–205)	45 (40–49)[a,b]
Male	108 (89–128)	106 (88–127)	186 (97–392)	44 (38–46)[a,b]
Female	98 (81–133)	98 (81–133)	97 (79–149)	45 (42–57)[a,b]
Basal LVEDD (mm)	67 ± 11	69 ± 10	53 ± 10[c]	47 ± 4[a,b]
Basal LVESD (mm)	59 ± 12	61 ± 11	43 ± 8[c]	32 ± 4[a,b]
LV sphericity (diastole)	0.68 ± 0.08	0.69 ± 0.08	0.62 ± 0.10[c]	0.55 ± 0.05[a,b]
EROA (mm^2)	30 (22–40)	30 (22–40)	24 (18–33)	NA
MR regurgitant volume (ml)	43 (31–54)	43 (32–55)	36 (25–52)	NA
MR regurgitant fraction (%)	47 ± 13	47 ± 13	42 ± 15	NA

[a] Ventricular FMR vs. controls, $p < 0.05$.
[b] Atrial FM vs. controls, $p < 0.05$.
[c] Ventricular FMR vs. atrial FMR, $p < 0.05$.

are presented in Table 3. Regarding chamber size, the multiple regression model demonstrated that only indexed LA volume was independently associated with MA area, irrespective of the presence or absence of AF. Male sex and age were also associated with increasing indexed MA area.

In controls, the MA displayed dynamism within the cardiac cycle, becoming smaller and more spherical in systole (diastolic vs. systolic area 8.4 ± 1.5 cm^2 vs. 8.0 ± 1.5 cm^2, $p = 0.04$; diastolic vs. systolic sphericity 0.69 ± 0.05 cm^2 vs. 0.73 ± 0.06 cm^2, $p < 0.01$). Mitral annular dynamism was diminished in both ventricular and atrial FMR, with no significant change in annular size or sphericity being observed between systole and diastole.

3.4. Mitral valve leaflet geometry

Table 4 details differences in mitral valve leaflet geometry was observed between controls, atrial and ventricular FMR. No absolute difference in leaflet lengths were observed between FMR and controls, however, both atrial and ventricular FMR subgroups demonstrated significantly shorter leaflets when indexed to SL distance. Compared to controls, both ventricular and atrial FMR exhibited a degree of leaflet tenting. However, in atrial FMR the extent of tenting was significantly less compared to ventricular FMR, manifested by a relatively smaller tenting area, height, and angles.

3.5. Papillary muscle geometry

Papillary muscle geometry amongst atrial and ventricular FMR and controls is compared in Table 5. In controls, the posteromedial papillary muscle (PMPM) head was located further apically relative to the MA plane in diastole, as compared to the anterolateral papillary muscle (ALPM) (25 ± 6 mm vs. 20 ± 3 mm, $p < 0.01$). In systole, there was significant shortening of the distance between PMPM head and MA plane (Δ 3.4 ± 3.1 mm, $p < 0.01$), whereas the distance between the ALPM head and MA plane remained unchanged (Δ 0.29 ± 2.2 mm, $p = 0.52$). There was significant reduction in inter-papillary muscle distance and total angle between papillary muscle heads in systole (diastole vs. systole 28 ± 6 mm vs. 21 ± 5 mm, $p < 0.01$; 67 ± 14° vs. 57 ± 14°, $p < 0.01$, respectively). The relative proportion given by the anterior and posterior angles to the total angle, however, remained constant throughout the cardiac cycle (anterior angle diastole vs. systole 59 ± 10% vs. 57 ± 14%, $p = 0.23$), Fig. 3).

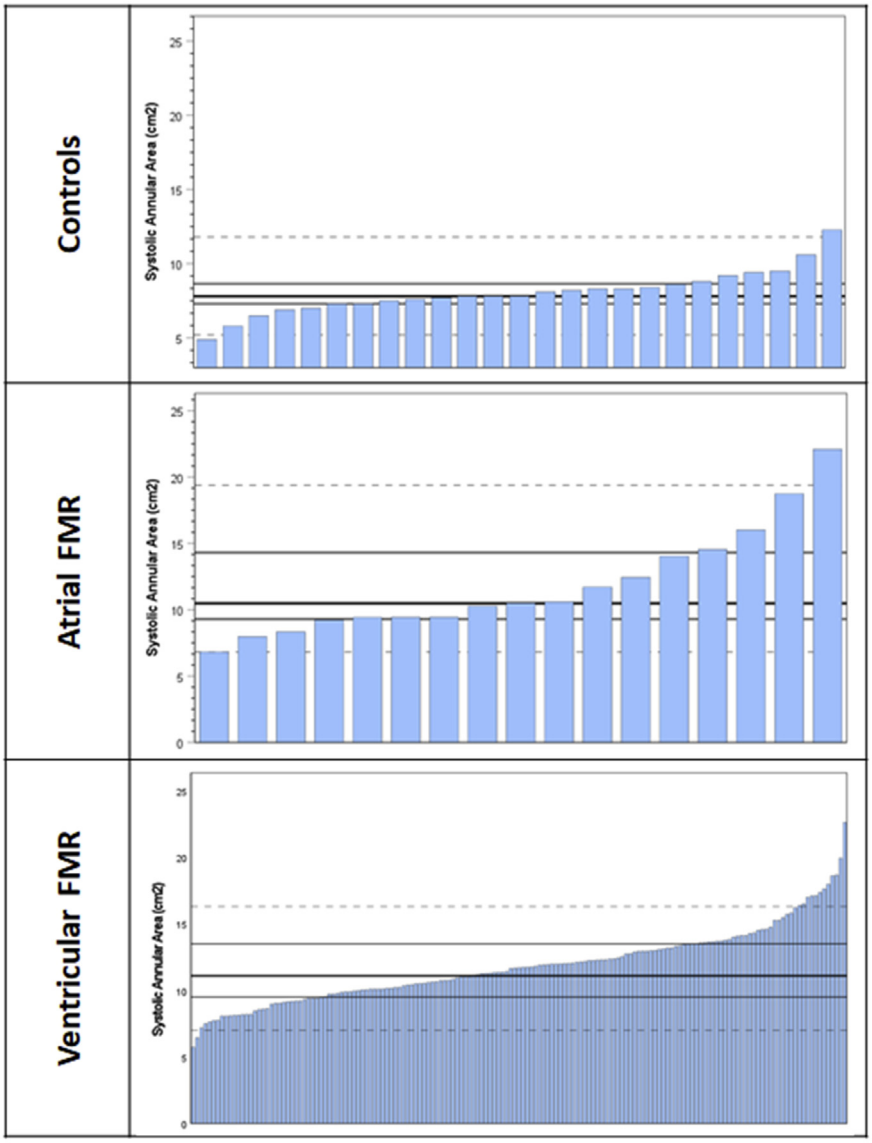

Fig. 4. Histogram depiction of mitral annular area in controls, atrial and ventricular FMR.

Table 2
Annular size in subgroups of FMR.

	Controls	Atrial FMR	Ventricular FMR
Systolic Total Perimeter (mm)	105 ± 10	125 ± 20	126 ± 14
Systolic IC Distance (mm)	36 ± 4	41 ± 7	41 ± 5
Systolic SL Distance (mm)	26 ± 3	33 ± 6	33 ± 4
Systolic Annulus Area (cm^2)	8.0 ± 1.5	11.9 ± 4.1	11.8 ± 3
Diastolic annular area/ LVEDV (cm^2/dl)	7.3 (6.5–7.8)	7.1 (5.9–10.0)[c]	4.2 (3.1–5.3)
Systolic annular area/LA Volume (cm^2/dl)	9.6 ± 2.3[a,b]	5.1 ± 1.8[c]	6.2 ± 1.6
Systolic Annular Sphericity	0.73 ± 0.06[a,b]	0.80 ± 0.05	0.80 ± 0.07
Diastolic Annular Sphericity	0.69 ± 0.05[a,b]	0.82 ± 0.07	0.81 ± 0.07

[a] Control vs. Atrial FMR $p < 0.05$.
[b] Control vs. Ventricular FMR $p < 0.05$.
[c] Atrial FMR vs. Ventricular FMR $p < 0.05$.

Similar to controls, ventricular FMR was characterised by relative apical positioning of the PMPM head. However, unlike controls, the mitral annular plane to PMPM head distance remained rather unchanged throughout the cardiac cycle (ventricular FMR vs. controls, 0.09 ± 3.68 mm vs. 3.4 ± 3.1 mm, $p < 0.01$). Additionally, the PMPM head was laterally displaced, with larger posterior papillary muscle angulation in both systole and diastole, and reduced change in total angulation with systole.

In contrast, no difference was observed in the papillary muscle geometry or dynamism between atrial FMR patients and controls, with maintained distances and angles in systole and diastole (Fig. 6).

4. Discussion

In the present study, using multiphasic cardiac CT, we have interrogated the geometrical differences within the mitral valve complex in atrial and ventricular functional mitral regurgitation, as they compare to controls. Crucially, we have shown that functional mitral regurgitation is a heterogeneous entity, with stark differences between atrial and ventricular FMR. We demonstrate that atrial FMR is predominantly

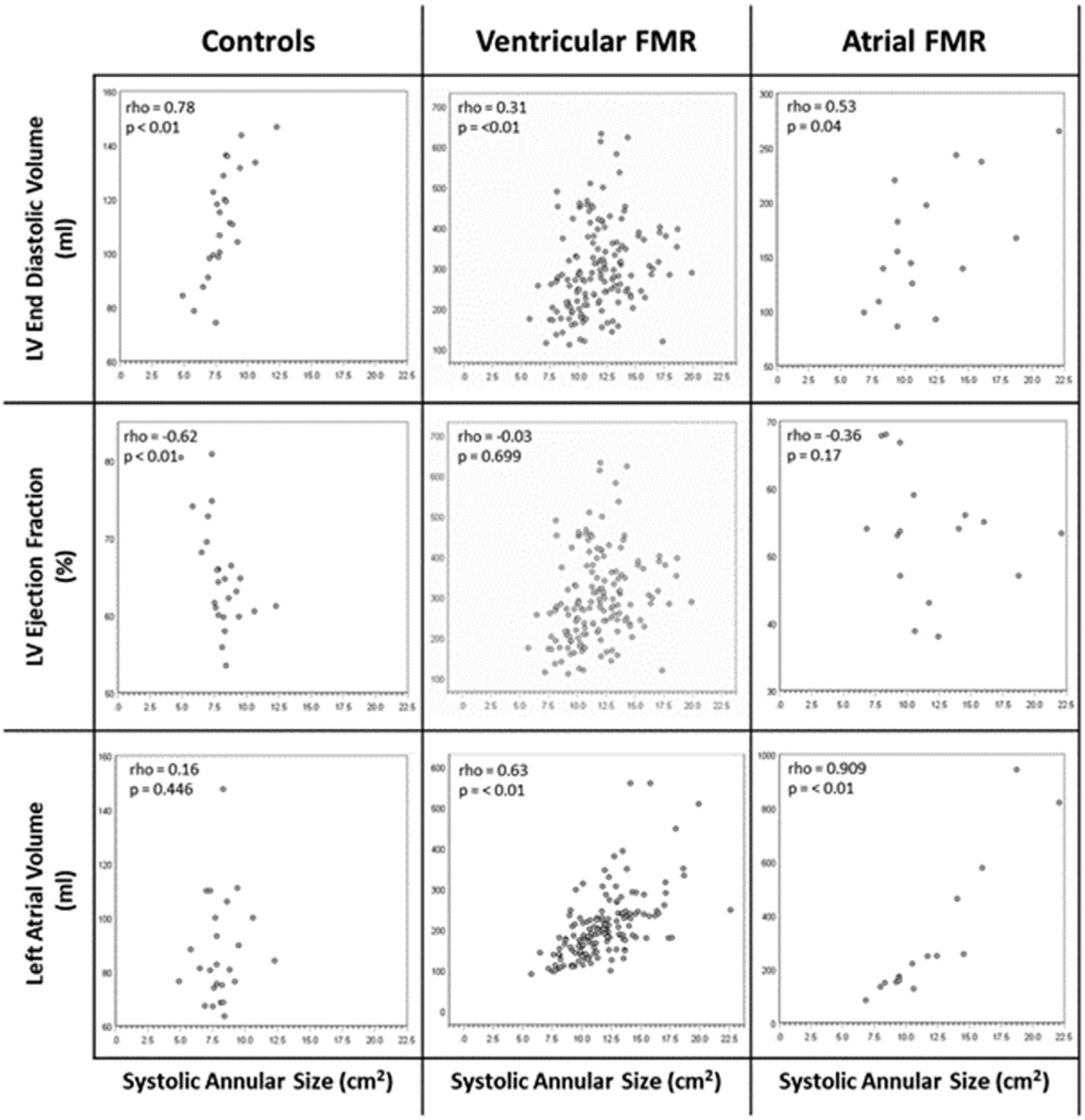

Fig. 5. Relationship between mitral annular size and atrioventricular remodelling in FMR and controls.

characterised by an enlarged and adynamic mitral annulus (which is related to both LV and LA dilatation), mitral valve tenting, but normal papillary muscle geometry. Ventricular FMR, however, is characterised by papillary muscle displacement and dysfunction, pronounced mitral valve tenting, and relatively less annular dilatation.

We identified a prevalence of aFMR of 10% in this otherwise unselected cohort of patients with FMR referred for consideration of TMVR. Whilst the difference in cohort size may generate difficulty in analysing differences in subgroups, the description alone is important. Unlike the overall prevalence of secondary MR, or the prevalence of significant MR in the context of atrial fibrillation, which are described, the burden of aFMR within cohorts of significant FMR is not clearly defined.[12–14]

In this study, we identify that both atrial and ventricular FMR, mitral annuli are on average larger, more spherical and adynamic compared to

Table 3
Univariate and multivariate predictors of mitral annulus area index in ventricular FMR.

	Univariate		B (SE)	Multivariate	
	R Value	p value		β	p value
Sex	0.276	<0.01	0.53 (0.17)	0.205	<0.01
Age	0.272	<0.01	0.02 (0.007)	0.210	<0.01
History of AF	0.207	<0.01	0.001 (0.176)	<0.01	0.996
Indexed LV End Diastolic Volume	0.045	0.291	–	–	–
LV Ejection fraction	0.006	0.471	–	–	–
Indexed LA Volume	0.533	<0.01	0.014 (0.002)	0.463	<0.01

Table 4
Differences in MV geometry in atrial and ventricular FMR.

	Controls	Atrial FMR	Ventricular FMR
AMVL Length (mm)	21.3 ± 3.8[b]	22.5 ± 4.4	23.2 ± 3.6[a]
PMVL Length (mm)	12.3 (11.4–14.0)	12.1 (11.3–16.7)	14.5 (13–16.8)
AMVL Length/SL	0.80 (0.72–0.87)[b]	0.72 (0.53–0.76)[a]	0.71 (0.63–079)
PMVL Length/SL	0.47 (0.45–0.57)[b]	0.39 (0.35–0.50)[a]	0.45 (0.40–0.51)
Tenting height (mm)	NA	6.9 ± 2.2	9.8 ± 3.4[c]
Tenting area (cm^2)	NA	0.61 (0.50–0.94)	1.46 (0.92–1.98)[c]
PMVL tenting angle (°)	NA	23 ± 13	43 ± 16[c]
AMVL tenting angle (°)	NA	16 ± 8	26 ± 13[c]

[a] Control vs. Atrial FMR $p < 0.05$.
[b] Control vs. Ventricular FMR $p < 0.05$.
[c] Atrial FMR vs. Ventricular FMR $p < 0.05$.

controls. Surprisingly, the absolute annular dimensions in those with atrial FMR were on average no different compared to ventricular FMR; furthermore, no statistically significant difference in indexed left atrial volume was observed between these groups. This may reflect the sex imbalance (despite volumes having been indexed to BSA). But the reason for this is difficult to interpret given the small number of patients. When indexed to LV size median annulus size was markedly larger in those with FMR compared to controls. However, when indexed to LA volume, MA

Table 5
Papillary muscle geometry in atrial FMR, ventricular FMR and controls.

	Controls		Atrial FMR		Ventricular FMR	
	Diastole	Systole	Diastole	Systole	Diastole	Systole
Anterolateral papillary muscle to annulus distance (mm)	20.2 ± 3.3	19.9 ± 4.1	18.7 ± 4.1	18.6 ± 4.0	20.8 ± 4.6	21.5 ± 4.6[c]
Posteromedial papillary muscle to annulus distance (mm	24.7 ± 5.7	21.3 ± 50[a,b]	22.9 ± 4.6	20.6 ± 4.5	25.8 ± 5.8	25.7 ± 5.8[c]
Papillary head-Papillary head distance (mm)	28.1 ± 5.7[b]	20.9 ± 4.7[a,b]	28.8 ± 5.8	22.5 ± 6.1[a]	36.3 ± 6.9[c]	32.2 ± 7.3[a,c]
Δ Anterolateral Pap muscle to annulus (mm)	0.29 ± 2.2		0.09 ± 1.96		−0.68 ± 3.02	
Δ Posteromedial Pap muscle to annulus (mm)	3.4 ± 3.1[b]		2.37 ± 4.8		0.09 ± 3.68[c]	
Δ Papillary head-Papillary head (mm)	7.2 ± 4.2[b]		6.2 ± 3.8		4.1 ± 4.1	
Anterior pap muscle angle (°)	39 ± 7	32 ± 8[a,b]	37 ± 9	33 ± 11[a]	41 ± 10	38 ± 9[a,c]
Posterior pap muscle angle (°)	28 ± 11[b]	25 ± 11[b]	33 ± 9	29 ± 8[a]	35 ± 10	32 ± 11[a]
Total angle (°)	67 ± 14[b]	57 ± 14[a,b]	71 ± 12	61 ± 14[a]	76 ± 14	71 ± 13[a,c]
AL angle proportion (%)	59 ± 10[b]	57 ± 14	53 ± 11	52 ± 12	54 ± 10	55 ± 11
Δ Anterior pap muscle angle (°)	5.5 (3.9–9.2)		2.9 (−0.9–6.2)		2.7 (−0.3–6.0)	
Δ Posterior pap muscle angle (°)	4.8 (−2.1–9.6)		4.8 (1.0–9.3)		1.9 (−1.4–6.7)	
Δ Total angle (°)	9.9 ± 13[b]		9.7 ± 11.7		4.8 ± 9	

[a] Control vs. Atrial FMR $p < 0.05$.
[b] Control vs. Ventricular FMR $p < 0.05$.
[c] Atrial FMR vs. Ventricular FMR $p < 0.05$.

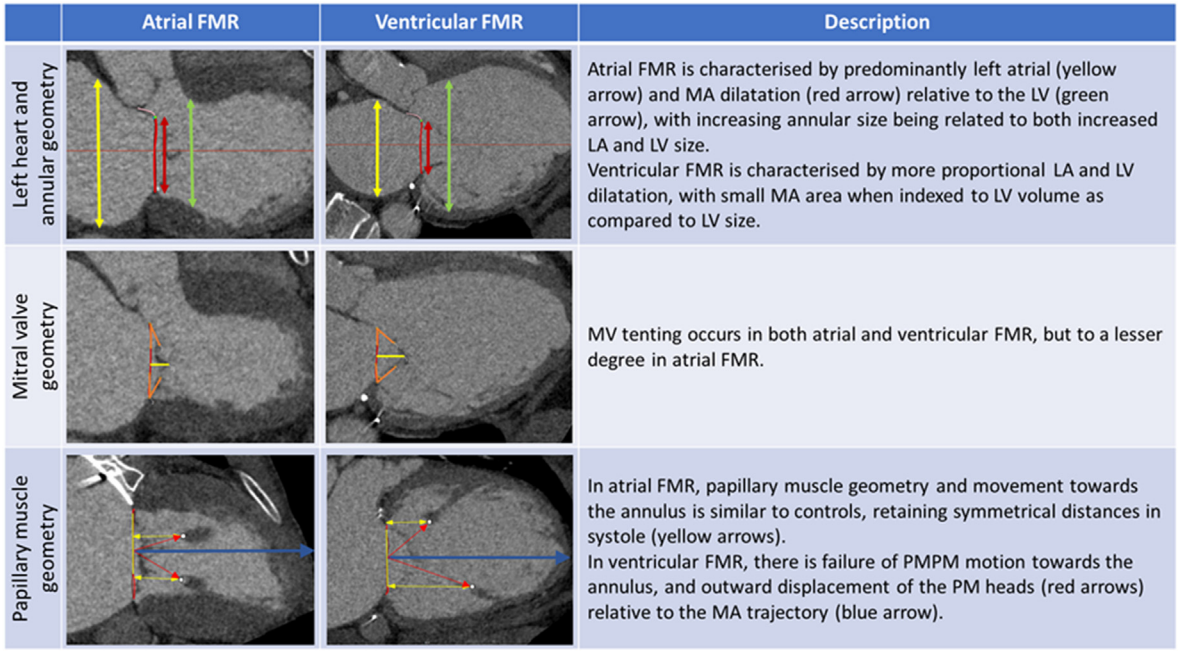

Fig. 6. Proposed geometrical differences between atrial and ventricular FMR.

area was significantly lower in both ventricular and atrial FMR compared to controls, particularly in atrial FMR. Taken together, this suggests that, despite larger LVEDV being a feature of atrial FMR compared to controls, it is not a driving factor in MA enlargement.

Enriquez-Sarano et al. have previously demonstrated the positive association of LA volume with LV enlargement, increasing severity of MR, degree of diastolic dysfunction, and presence of AF, in patients with dilated cardiomyopathy, with maximal LA volume being an independent predictor of mortality.[15] Our group has previously reported that both LA and LV sizes contribute to MA size in controls, however analysis of patients with FMR was limited by small cohort size.[8] Our larger cohort of patients with ventricular FMR has provided deeper insight into the relationships between chamber size and MA area, identifying that MA dimensions were related to indexed LA volume, but not LV size. Interestingly, age and male sex were also independently associated with increasing MA area, which was not observed in the previously published data.[8] When indexed to LV volume, MA area in patients with ventricular FMR was significantly smaller than aFMR and controls, which were similar. When indexed to LA volume, MA area was significantly lower in both ventricular and atrial FMR compared to controls, particularly in atrial FMR. Taken together, this suggests that, despite larger LVEDV being a feature of atrial FMR compared to controls, it is not a driving factor in MA enlargement.

Patients with AF and aFMR have larger LA and MA,[4] all of which have the potential to regress if the cycle of AF and progressive LA dilatation is stopped by rhythm control. Interestingly, the presence of AF was not found to be an independent predictor of annular size in patients with ventricular FMR. There are large disparities in clinical practice between the degree of MR observed for similar annular dilatation,[12] the reasons for which are not completely understood. Otsuji et al. have suggested that similar degrees of MA dilatation within patients with atrial or ventricular FMR resulted in only mild mitral regurgitation in the atrial group, compared to moderate-to-severe in the ventricular group.[16]In our study, increasing MA area was univariately associated with increasing LA volume and LVESV, in vFMR, however it is important to recognise that the latter may be confounded by the presence of severe MR. The small and selected cohort limited multivariate analysis of predictors of MA size in patients with aFMR.

In healthy individuals, the area of the mitral valve leaflets must be sufficient to cover the annular area with a leaflet-to-closure area ratio >1.7 being required to prevent significant MR.[17] Studies using 3DE have reported the immense capacity of the MV leaflets for remodelling, increasing in size by ~30–45% in the face of LV and annular dilatation. Inadequate leaflet remodelling is associated with the development of FMR.[17–19] Similar intricate 3D evaluation of leaflet area and closure area is, as yet, not routine with CT. In the present study, we used absolute leaflet lengths, and lengths referenced to SL distance, as simplified surrogate markers of leaflet remodelling. Whilst no statistically significant difference in either measure was observed between atrial FMR and ventricular FMR, absolute leaflet lengths of the anterior mitral valve leaflet (AMVL) and PMVL were increased in ventricular FMR compared to controls. Referenced lengths, however, were significantly reduced in both atrial and ventricular FMR. Overall, these findings are likely reflective of the, albeit inadequate, remodelling process, particularly both atrial and ventricular FMR.

In ventricular FMR, LV remodelling and PM displacement increases MV leaflet tension that tethers the leaflets resulting in systolic tenting and insufficient coaptation.[20–22] The degree of tenting has been shown to be an independent predictor of MR severity, prognosis, and recurrence of MR after annuloplasty[23–25] and can be assessed by CT as demonstrated in this analysis as well as by others previously.[26] Historically, atrial FMR has been considered the leading cause of Carpentier type I MR, implying normal leaflet motion.[27] However, Kim et al. have demonstrated a degree of leaflet tethering using 3DE in AF, with greater degrees of tenting being seen in those with MR, compared to those without.[4] Silbiger has proposed 'atriogenic' leaflet tethering as an additional mechanism in the generation of MR in atrial dilatation, describing posterior translocation of the MA to the outside of the very basal posterior myocardium, thereby restricting leaflet motion.[5] Tenting height, area and angle were not determinable in our controls as the leaflets were seen to rest just at the level of the annular plane during systole. Whilst the degree of tenting was lower in atrial FMR compared to previous echocardiographic reports of normal values,[28] it was, however, discernible, unlike controls, implying that a) CT-derived and echocardiographically-derived measurements are not interchangeable and b) an abnormal degree of tenting was present in the atrial FMR group.

Knowledge of papillary muscle geometry is required to determine whether the leaflet tethering seen in atrial FMR is atriogenic in isolation. Consistent with previous animal models, and studies using 3DE, we found that ventricular FMR was associated with apical displacement and restriction of the posteromedial papillary muscle,[29–32] but rather being a feature typified by inferolateral regional infarct, as could be conceptualized, this phenomenon was seen in our unstratified group of patients with ventricular FMR, which will need further analysis. Kim et al. have also determined that lateral displacement of the PMs relative to the centre of the ventricle contributes to symmetrical tethering, predominantly in non-ischemic dilated cardiomyopathy.[33] Lateral papillary muscle displacement, evidenced by increased systolic PM-PM head distance, increased systolic total angle between PM heads, and reduced total angle shortening in systole, was seen throughout subgroups of ventricular FMR. Within subgroups, inferolateral MI patients demonstrated less papillary muscle apposition, despite similar degrees of fractional shortening. In comparison, atrial FMR patients displayed no statistically significant differences in apical or outward PM displacement, consistent with the overall preservation of ventricular size and function, and the concept of atriogenic tethering.

FMR, as described in prior literature and the data presented in this study, is driven by an interplay of factors: annular dimensions, leaflet lengths (absolute and relative to annular size), coaptation length, tenting, papillary muscle geometry, pressure and volume loading, LV end-diastolic pressure and LA pressure). As expected, annular area is related to LA volume; in aFMR, annular size is bigger and therefore relative leaflet length is less. Tenting height and volume is greater in vFMR, whilst changes in papillary muscle architecture are not obvious in aFMR. Whilst the findings in this study are valuable to further our understanding of the geometrical differences between atrial and ventricular FMR, there are still uncertainties regarding the pathophysiological cascade driving MR, of differing severities, in the presence of otherwise seemingly similar grades of atrial or ventricular disease. In order to define these pathways, and therefore the most appropriate timepoint and methods of targeted intervention, a more temporal study of these the interplay of these geometrical differences as predictors of the development of MR with clinical factors in a broader cohort of patients with LV and atrial dysfunction is needed.

Once a patient with FMR is being considered for MV-targeted intervention, an understanding of these geometric findings, particularly given the range of percutaneous options potentially available, is important. Given that by its very nature, FMR is predominantly a disorder of geometrical distortion of either the LA, annulus, or LV and subvalvular apparatus, unless the underlying cause of secondary valve dysfunction is tackled to mitigate against disease progression, or the intervention targets the specific mechanism of regurgitation, long-term procedural success cannot be guaranteed. For example, progressive LV remodelling will only induce further papillary muscle dysfunction and leaflet tethering,[34] explaining high recurrence rates after successful annuloplasty[35] and MitraClip.[36] It could be postulated that a patient with predominantly aFMR, where the predominant issue is that of annular dilatation and small leaflets relative to the annulus, would have a better procedural result with a device targeting the annulus as opposed to edge-to-edge repair, alone, as the progressive element of the disease, i.e., annular dilatation has not been addressed. Successful annular remodelling with annuloplasty for atrial FMR may be beneficial,[37] however further study is

needed to determine the long-term impact on MR, over and above a rhythm control strategies and medical optimization.

Having a means of exploring this concept, as this study demonstrates CT is capable of providing, is important for future study of both aFMR and vFMR. Quite simply, FMR is too heterogeneous a disease to suggest that there is a one-size-fits-all approach to therapy selection, and to our understanding of outcomes with therapy.

Recent data suggests better medium- and longer-term survival in patients with atrial FMR compared to ventricular FMR undergoing surgical MV intervention, highlighting the importance of granular discrimination between these two entities to facilitate more individualised approach to management.[38]

5. Limitations

The sample size of patients with atrial FMR was small, with selection bias of patients with advanced LV dysfunction and ventricular FMR, and a control cohort of a different age compared to cases. It does not explore difference in patients with advanced LV impairment and no, or little, FMR, or patients with lesser degrees of aFMR. In the context of a small sample size (although appropriately proportional to our experience of the amount of significant aFMR seen in our clinical practice), the findings described cannot be definitive. We acknowledge that this study is largely hypothesis generating, but importantly demonstrates how CT can explore geometrical differences such as this, arguably in a way that no other modality could do with ease. We have demonstrated that CT may be used as a complimentary, non-invasive tool in the comprehensive geometric assessment of FMR. Echocardiography has higher temporal resolution, with high frame rates conveying a greater ability to determine subtle geometric changes within the cardiac cycle, which is crucial in the correlation of these changes to the timing within systole of regurgitation. It is also important to acknowledge that the measurements taken at the same time point in the cardiac cycle may not be directly comparable between cases and controls. For example, in ischemic MR, the mitral annulus area has been demonstrated to be larger in the early - mid diastole compared with end-systole.[39] Increasing the number of phases to enhance temporal resolution would allow for more definitive exploration of the appropriate phase for analysis. For example, a 'simplified' measure of mitral annular dynamism is provided in this paper, and quantification of MV annular size is limited to end systole and diastole which may miss bigger or smaller sizes which may alter dynamism findings. Nevertheless, with its ability for unlimited, whole heart multiplanar reconstruction and high spatial resolution, CT provides the opportunity to scrutinize geometrical relationships throughout the mitral valve apparatus.

6. Conclusion

Both ventricular and atrial FMR are complex disorders, comprising multifactorial pathologies that contribute to regurgitation. Our findings suggest that, despite the absence of primary leaflet disease, the atrial and ventricular FMR differ in their underlying geometrical pathologies, and potentially should be considered differently in terms of clinical decision making and outcomes.

Funding

None.

Declaration of competing interest

Dr Blanke and Dr Leipsic provide CT core laboratory (University of British Columbia) for Edwards LifeSciences, Abbott and Medtronic with no personal compensation. Dr. Blanke is a consultant to Edwards LifeSciences, Gore, Circle Cardiovascular Imaging, and Neovasc. Dr Leipsic is consultant with stock options for Circle Cardiovascular Imaging. Dr Webb is a consultant to Edwards LifeSciences.

References

1. Trichon BH, Felker GM, Shaw LK, Cabell CH, O'Connor CM. Relation of frequency and severity of mitral regurgitation to survival among patients with left ventricular systolic dysfunction and heart failure. *Am J Cardiol*. 2003;91(5):538–543.
2. Otsuji Y, Handschumacher MD, Schwammenthal E, et al. Insights from three-dimensional echocardiography into the mechanism of functional mitral regurgitation: direct in vivo demonstration of altered leaflet tethering geometry. *Circulation*. 1997 Sep 16;96(6):1.
3. Fan Y, Wan S, Wong RH, Lee AP. Atrial functional mitral regurgitation: mechanisms and surgical implications. *Asian Cardiovasc Thorac Ann*. 2020 Sep;28(7):421–426.
4. Kim DH, Heo R, Handschumacher MD, et al. Mitral valve adaptation to isolated annular dilation: insights into the mechanism of atrial functional mitral regurgitation. *JACC Cardiovasc Imag*. 2019;12(4):665–677.
5. Silbiger JJ. Does left atrial enlargement contribute to mitral leaflet tethering in patients with functional mitral regurgitation? Proposed role of atriogenic leaflet tethering. *Echocardiography*. 2014;31(10):1310–1311.
6. Kagiyama N, Hayashida A, Toki M, et al. Insufficient leaflet remodeling in patients with atrial fibrillation: association with the severity of mitral regurgitation. *Circ Cardiovasc Imag*. 2017 Mar;10(3), e005451.
7. Stone GW, Lindenfeld J, Abraham WT, et al. Transcatheter mitral-valve repair in patients with heart failure. *N Engl J Med*. 2018 Dec 13;379(24):2307–2318.
8. Naoum C, Leipsic J, Cheung A, et al. Mitral annular dimensions and geometry in patients with functional mitral regurgitation and mitral valve prolapse implications for transcatheter mitral valve implantation. *JACC Cardiovasc Imag*. 2016;9(3):269–280.
9. Zoghbi WA, Adams D, Bonow RO, et al. Recommendations for noninvasive evaluation of native valvular regurgitation: a report from the American society of echocardiography developed in collaboration with the society for cardiovascular magnetic resonance. *J Am Soc Echocardiogr*. 2017 Apr;30(4):303–371.
10. Blanke P, Naoum C, Webb J, et al. Multimodality imaging in the context of transcatheter mitral valve replacement establishing consensus among modalities and disciplines. *JACC (J Am Coll Cardiol): Cardiovasc Imag*. 2015;8:1191–1208.
11. Delgado V, Tops LF, Schuijf JD, et al. Assessment of mitral valve anatomy and geometry with multislice computed tomography. *JACC Cardiovasc Imag*. 2009;2(5):556–565.
12. Deferm S, Bertrand PB, Verbrugge FH, et al. Atrial functional mitral regurgitation: JACC review topic of the week. *J Am Coll Cardiol*. 2019;73(19):2465–2476.
13. de Marchena E, Badiye A, Robalino G, et al. Respective prevalence of the different carpentier classes of mitral regurgitation: a stepping stone for future therapeutic research and development. *J Card Surg*. 2011;26(4):385–392.
14. Gertz ZM, Raina A, Saghy L, et al. Evidence of atrial functional mitral regurgitation due to atrial fibrillation: reversal with arrhythmia control. *J Am Coll Cardiol*. 2011;58(14):1474–1481.
15. Rossi A, Cicoira M, Zanolla L, et al. Determinants and prognostic value of left atrial volume in patients with dilated cardiomyopathy. *J Am Coll Cardiol*. 2002 Oct 16;40(8):1425–1430.
16. Otsuji Y, Kumanohoso T, Yoshifuku S, et al. Isolated annular dilation does not usually cause important functional mitral regurgitation. *J Am Coll Cardiol*. 2002;39(10):1651–1656.
17. Chaput M, Handschumacher MD, Tournoux F, et al. Mitral leaflet adaptation to ventricular remodeling occurrence and adequacy in patients with functional mitral regurgitation. *Circulation*. 2008;118(8):845–852.
18. Marsit O, Clavel MA, Côté-Laroche C, et al. Attenuated mitral leaflet enlargement contributes to functional mitral regurgitation after myocardial infarction. *J Am Coll Cardiol*. 2020;75(4):395–405.
19. Debonnaire P, Al Amri I, Leong DP, et al. Leaflet remodelling in functional mitral valve regurgitation: characteristics, determinants, and relation to regurgitation severity. *Eur Heart J Cardiovasc Imag*. 2015;16(3):290–299.
20. He S, Fontaine AA, Schwammenthal E, Yoganathan AP, Levine RA. Integrated mechanism for functional mitral regurgitation. *Circulation*. 1997;96(6):1826–1834.
21. Agricola E, Oppizzi M, Maisano F, et al. Echocardiographic classification of chronic ischemic mitral regurgitation caused by restricted motion according to tethering pattern. *Eur J Echocardiogr*. 2004;5(5):326–334.
22. el Sabbagh A, Reddy YNV, Nishimura RA. Mitral valve regurgitation in the contemporary era. *JACC (J Am Coll Cardiol): Cardiovasc Imag*. 2018 Apr;11(4):628–643.
23. Nappi F, Lusini M, Avtaar Singh SS, Santana O, Chello M, Mihos CG. Risk of ischemic mitral regurgitation recurrence after combined valvular and subvalvular repair. *Ann Thorac Surg*. 2019;108(2):536–543.
24. Karaca O, Avci A, Guler GB, et al. Tenting area reflects disease severity and prognosis in patients with non-ischaemic dilated cardiomyopathy and functional mitral regurgitation. *Eur J Heart Fail*. 2011;13(3):284–291.
25. Von Stumm M, Dudde F, Gasser S, et al. Prognostic value of mitral valve tenting area in patients with functional mitral regurgitation. *Interact Cardiovasc Thorac Surg*. 2020;30(3):431–438.
26. Beaudoin J, Thai WE, Wai B, Handschumacher MD, Levine RA, Truong QA. Assessment of mitral valve adaptation with gated cardiac computed tomography: validation with three-dimensional echocardiography and mechanistic insight to functional mitral regurgitation. *Circ Cardiovasc Imag*. 2013;6(5):784–789.
27. Carpentier A. Cardiac valve surgery: the 'French correction'. *J Thorac Cardiovasc Surg*. 1983;86(3):323–337.
28. Dudzinski DM, Hung J. Echocardiographic assessment of ischemic mitral regurgitation. *Cardiovasc Ultrasound*. 2014;12:46.
29. Kim K, Kaji S, An Y, et al. Mechanism of asymmetric leaflet tethering in ischemic mitral regurgitation: 3D analysis with multislice CT. *JACC (J Am Coll Cardiol): Cardiovasc Imag*. 2012;5(2):230–232.

30. Yamaura Y, Watanabe N, Ogasawara Y, et al. Three-dimensional echocardiographic measurements of distance between papillary muscles and mitral annulus: assessment with three-dimensional quantification software system. *J Echocardiogr*. 2008;6:67–73.
31. Tibayan FA, Rodriguez F, Zasio MK, et al. Geometric distortions of the mitral valvular-ventricular complex in chronic ischemic mitral regurgitation. *Circulation*. 2003;108(10 SUPPL):116–121.
32. Kimura T, Roger VL, Watanabe N, et al. The unique mechanism of functional mitral regurgitation in acute myocardial infarction: a prospective dynamic 4D quantitative echocardiographic study. *Eur Heart J Cardiovasc Imag*. 2019;20(4):396–406.
33. Kim K, Kaji S, An Y, et al. Interpapillary muscle distance independently affects severity of functional mitral regurgitation in patients with systolic left ventricular dysfunction. *J Thorac Cardiovasc Surg*. 2014;148(2):434–440.
34. Hung J, Papakostas L, Tahta SA, et al. Mechanism of recurrent ischemic mitral regurgitation after annuloplasty: continued LV remodeling as a moving target. *Circulation*. 2004;110(11 Suppl 1):II85–II90.
35. Acker MA, Parides MK, Perrault LP, et al. Mitral-valve repair versus replacement for severe ischemic mitral regurgitation. *N Engl J Med*. 2014;370(1):23–32.
36. Ikenaga H, Makar M, Rader F, et al. Mechanisms of mitral regurgitation after percutaneous mitral valve repair with the MitraClip. *Eur Heart J Cardiovasc Imag*. 2019;1:1–13.
37. Takahashi Y, Abe Y, Sasaki Y, et al. Mitral valve repair for atrial functional mitral regurgitation in patients with chronic atrial fibrillation. *Interact Cardiovasc Thorac Surg*. 2015;21(2):163–168.
38. Hirji SA, Cote CL, Javadikasgari H, Malarczyk A, McGurk S, Kaneko T. Atrial functional versus ventricular functional mitral regurgitation: prognostic implications. *J Thorac Cardiovasc Surg*. 2020;377:1847. https://doi.org/10.1016/j.jtcvs.2020.12.098.
39. Daimon M, Saracino G, Fukuda S, et al. Dynamic change of mitral annular geometry and motion in ischemic mitral regurgitation assessed by a computerized 3D echo method. *Echocardiography*. 2010 Oct;27(9):1069–10677.34.